Fe3O4@polydopamine Nanoparticle-Labeled Umbilical Cord Mesenchymal Stem Cells Arrest Intervertebral Disc Degeneration by Enhancing Cell Migration

Meng Zhang
China-Japan Union Hospital of Jilin University
Butain Zhang
China-Japan Union Hospital of Jilin University
Ran Li
China-Japan Union Hospital of Jilin University
Te Liu
China-Japan Union Hospital of Jilin University
Jun Zhang
China-Japan Union Hospital of Jilin University
Ying Wang
China-Japan Union Hospital of Jilin University
Fuqiang Zhang
China-Japan Union Hospital of Jilin University
Xupeng Mu (muxupeng@jlu.edu.cn)
China-Japan Union Hospital of Jilin University
Jinlan Jiang
China-Japan Union Hospital of Jilin University

Research

Keywords: Umbilical cord mesenchymal stem cells, Intervertebral disc degeneration, Migration, Fe3O4@polydopamine nanoparticle

Posted Date: January 18th, 2021

DOI: https://doi.org/10.21203/rs.3.rs-147494/v1

Abstract

Cell therapies for intervertebral disc degeneration (IDD) are intended to replace lost intervertebral disc (IVD) cells. The key to this treatment is to promote the migration of transplanted cells to the lesion site. The purpose of this study was to evaluate the repair effect of umbilical cord mesenchymal stem cells (UCMSCs) labeled with Fe_3O_4@polydopamine nanoparticles (Fe_3O_4@PDA NPs) on rat caudal vertebra disc degeneration. We characterized UCMSCs labeled with Fe_3O_4@PDA NPs, analyzed the effects of nanoparticles on UCMSCs and evaluated UCMSCs labeled with Fe_3O_4@PDA NPs to repair IDD in vivo. We found that UCMSC Fe_3O_4@PDA NPs could enhanced the migration of UCMSCs by up-regulating the expression of CXC chemokine receptor type 4 (CXCR4) without effecting UCMSC functionality and the Fe_3O_4@PDA NPs-labeled UCMSC group had better disc height, better tissue morphology performance and a higher number of transplanted cells and induced notably better regeneration of IVD, evidenced by the higher expression of aggrecan, type II collagen, and Sox-9 and lower expression of Mmp-13, Tnf-α and Il-1β at both mRNA and protein levels than the unlabeled group. We demonstrated systemic delivery of UCMSCs labeled with Fe_3O_4@PDA NPs could be an appropriate protocol for accelerating and optimizing clinically applicable UCMSC treatment for IDD.

1. Background

Intervertebral disc degeneration (IDD) is characterized by a decrease in the number of nucleus pulposus cells and abnormalities in the fibrous ring structure, followed by the disruption of the balance between matrix anabolism and catabolism.[1,2] The reduction of water content, glycoprotein, and type II collagen in the intervertebral disc (IVD) leads to changes in the structure and morphology of the IVD. These changes eventually affect the function of the IVD and cause lower back pain, which brings huge treatment costs, causing a serious economic burden.[3] Pharmacological treatment and surgery can relieve symptomatic pain of IDD but fail to reverse disc degeneration.[4] Therefore, various kinds of biological therapeutic methods have been studied in the hope of regenerating the dysfunctional discs.[5] Among these methods, stem cell therapy is of high interest.[6]

Due to the extensive tissue distribution of mesenchymal stem cells (MSCs), along with their pluripotency and non-immunogenicity, they play an important role in damaged tissue repair, which makes MSCs attractive for IVD regeneration.[7] In vitro, co-culture of MSCs and IVD cells can differentiate into nucleus pulposus-like cells and synthesize glycosaminoglycans and type II collagen.[8] In vivo, MSCs are capable of differentiating into nucleus pulposus-like cells, increasing the extracellular matrix (ECM), as well as disc hydration, disc height, and glycosaminoglycan production.[9] Compared with other types of cells for transplantation, umbilical cord mesenchymal stem cells (UCMSCs) have several advantages.[10] UCMSCs are derived from umbilical cord discarded after birth. Separation and cultivation are simple and effective, which do not require an invasive procedure.[11] In addition, UCMSCs can expand in vitro and still retain pluripotency after many generations of expansion.[12] However, in most previous studies, MSCs were

transplanted to the degenerative disc site through invasive intradiscal injection. During intradiscal injection, it is necessary to enter the nucleus pulposus cavity through annulus fibrosus, but this process destroys the physiological structure of the disc that causes disc degeneration.[13] This local transplantation effect relies on MSCs to differentiate into IVD-like cells to repair the damaged tissue.[14] However, the microenvironment of the IVD tissue includes low oxygen, low nutrition, acidic pH and high mechanical load, which poses a huge threat to the survival of stem cells.[15] Also, cell leakage remains a side effect to be considered when using intradiscal injection.[16]

More recently, some studies have addressed the role of MSCs in the injury site homing following intravenous injection.[17] Utilizing the homing ability of systemically delivered MSCs can bypass the increased complications associated with intradiscal injection into the IVD. In bovine whole organ culture, MSC recruitment occurs in response to IVD degrading conditions.[18] A study comparing intravenous stem cells to intradiscal disc stem cells showed that regardless of the delivery method used, MSC implantation is not observed at the injured site. Both delivery methods increase the expression of glycosaminoglycan (GAG) and *Acan*, suggesting that there may be paracrine effects.[19] Another study proved that systemic perfusion of MSCs in the mouse disc degeneration group increases the number of stem cell transplantation in endplates, fibrous rings, and even the NP compared with the normal control group.[20] Cunha et al. found that systemic transplantation of MSCs has a beneficial effect on IVD regeneration in situ, and stated that tissue regeneration is achieved through complex interactions between stromal cells and immune system cells.[21] Although the exact mechanism of MSCs homing to damaged tissues has not been resolved, there is increasing evidence that chemokines and their receptors are important factors in controlling cell migration.[22] In particular, interactions between stromal cell-derived factor-1α (SDF-1α, also known as CXC motif chemokine 12, CXCL12) and its receptor CXC chemokine receptor type 4 (CXCR4) are essential in this process.[23] Additionally, hepatocyte growth factor, via interactions with its receptor c-met, and monocyte chemoattractant protein-1 (MCP-1), via interactions with chemokine receptor 2 (CCR2), are involved in stem cell migration[24]. However, the expression levels of these receptors are low in MSCs in vitro expansion.[25] Therefore, systemic delivery of MSCs can repair damaged intervertebral tissue, but significant challenges remain in effectively implanting them into the target site to enhance successful implantation.[26] Promoting and improving cell homing remains a major challenge in regenerative medicine.

Nanotechnology and nanoparticles (NPs) are widely used in regenerative medicine and have good potential in the diagnosis and treatment of different diseases.[27] One nanoparticle is iron oxide (Fe_3O_4), which has been widely used as a contrast agent and drug carrier in preclinical and clinical environments.[28] Due to its good biocompatibility and response to magnetic fields, many studies have recently used it as a tracer for stem cells.[29] Some studies have shown that NPs do not alter the viability, proliferation, phenotype, function, and migration characteristics of MSCs in vitro.[30] However, some other studies suggest that Fe_3O_4 nanoparticle labeling does not affect stem cell viability, differentiation, and proliferation, but improves stem cell migration to tumor, inflammation, and degenerative disease sites.[31]

Although the molecular mechanism by which Fe_3O_4 nanoparticle-labeled MSCs have enhanced migration capacity has not been elucidated, it has been suggested that Fe_3O_4 nanoparticles enhance stem cell migration by up-regulating the expression of CXCR4 on MSCs.[32] Increasing evidence shows that cell responses to Fe_3O_4 nanoparticles have indeed been observed, although the inherent characteristics of Fe_3O_4 nanoparticle-labeled MSCs have not been fully explored.[33]

Therefore, the strategy of using Fe_3O_4 nanoparticles to enhance stem cell migration capacity can improve the effectiveness of stem cell therapy.[34] In this study, we synthesized polydopamine-capped Fe_3O_4 (Fe_3O_4@PDA) and explored the role of UCMSCs labeled with NPs in enhancing stem cell regeneration in disc degeneration (Fig. 1A). Moreover, we tested our hypothesis that Fe_3O_4@PDA NPs stem cell labeling strategies to increase their migration capacity optimize IDD therapy.

2. Materials And Methods

2.1 Reagents

Iron acetylacetonate (Fe(acac)3, 99.9%), 1,2-hexadecanediol (90%), benzyl ether (99%), oleyamine (OLA, 70%), oleic acid (OA, 90%), sodium dodecyl sulfate (SDS, 99%), dopamine hydrochloride (DA,99.0%), tris (hydroxymethyl) aminomethane (Tris) (99.0%), 3H-Indolium,5-[[[4-(chloromethyl)benzoyl]amino]methyl]-2-[3-(1,3-dihydro-3,3-dimethyl-1-octadecyl-2H-indol-2-ylidene)-1-propenyl]-3,3-dimethyl-1-octadecyl-,chloride (CM-Dil) and Cell Counting Kit-8 (CCK-8) were purchased from Sigma-Aldrich (Louis, MO, USA).. Dulbecco's Modified Eagle's Medium with high glucose and fetal bovine serum (FBS) were purchased from Thermo Fisher Scientific (Waltham, MA, USA). Other reagents (analytical grade) were purchased from Beijing Chemical Reagents Company (Beijing, China) unless otherwise stated.

2.2 Fe_3O_4 nanoparticle synthesis

Fe_3O_4@PDA nanoparticles (Fe_3O_4@PDA NPs) were synthesized as previously described.[35] Briefly, 2 mmol of $Fe(acac)_3$, 5 mmol of 1,2-hexadecanediol, 6 mmol of OA, and 6 mmol of OLA were mixed in 20 mL of benzyl ether. After the mixture was stirred for 15 min under nitrogen-containing atmosphere, the OA-stabilized Fe_3O_4 NPs were obtained. Precisely 4.0 mL of OA-stabilized Fe_3O_4 NPs (7.0 mg/mL) was added to SDS aqueous solution (14 mg/mL, 12.5 mL) under mechanical stirring and nitrogen-containing atmosphere at room temperature. After ultrasonic treatment, the emulsion was further heated at 60 °C to evaporate toluene and obtain SDS-capped Fe_3O_4 NPs. SDS-capped Fe_3O_4 NPs were centrifuged and dispersed in Tris-buffer solution (10 mM, pH 8.5) and then DA monomer was added. After stirring for 3 h, PDA-capped Fe_3O_4 NPs were obtained. The products were washed through centrifugation to discard the extra self-polymerized DA in the solution. Lastly, the Fe_3O_4@PDA NPs were obtained by centrifugation at 10,000 rpm for 10 min and washed with deionized water. Fe_3O_4@PDA NPs (100 μg/mL) were detected using a Hitachi H-800 electron microscope (Hitachi Co., Ltd., Tokyo, Japan) with a charge-coupled device camera at an acceleration voltage of 200 kV.

2.3 Cell culture

UCMSCs were purchased from American Type Culture Collection (Manassas, VA, USA). UCMSCs were cultured in DMEM α supplemented with 10% FBS in a humidified atmosphere of 5% CO_2 at 37 °C. When the cells adhered to reach 80% confluence in the culture flask, the cells were passaged. The antibody cocktails (BD Stemflow™, San Diego, CA, USA) were used for flow cytometry analysis. The MSC positive cocktail (FITC CD90, PerCP-Cy™5.5 CD105 and APC CD73) left the PE channel open for use in combination with the supplied negative MSC cocktail (PE CD45, PE CD34, PE CD11b, PE CD19 and PE HLA-DR).

2.4 Prussian blue staining

UCMSCs were grown at 80% confluency and incubated with Fe_3O_4@PDA NPs at different concentrations (0, 25, 50, 75, 100, and 150 μg/mL) for 24 h. UCMSCs were washed three times with PBS and stained using Prussian Blue Iron Staining Kit (Solarbio, Beijing, China) according to the manufacturer's instructions.

2.5 Fe quantification in UCMSCs

When UCMSCs were incubated with Fe_3O_4@PDA NPs for 24 h, 1×10^6 cells were collected. Cells were then dissolved in 0.3 mL of concentrated nitric acid (~ 70%) and 0.1 mL of hydrogen peroxide (30%). Iron concentration was determined using inductively coupled plasma optical emission spectrometer (ICP-OES) (PerkinElmer, Norwalk, USA).

2.6 Transmission electron microscopy (TEM) of Fe_3O_4@PDA NP localization in UCMSCs

We used TEM to assess the uptake and localization of Fe_3O_4@PDA NPs s by UCMSCs and their possible influence on cell ultrastructure. MSCs treated with Fe_3O_4@PDA NPs (50 μg/mL) were washed twice with PBS and fixed in phosphate-buffered Karnofsky's solution, followed by staining with 2% osmiumtetroxide at 4 °C overnight. Then cells were scraped off the plastic and dehydrated in an ethanol series. The specimens were embedded in Araldite (Serva). Ultrathin sections were established using an ultramicrotome (Leica, Bensheim, Germany), mounted on pioloform-coated copper grids, stained with uranyl acetate and lead hydroxide, and analyzed using a Tecnai Spirit system (120 kV; FEI, Hillsboro, OR, USA).

2.7 Effects of Fe_3O_4@PDA NPs on UCMSC viability and proliferation

CCK-8 assay was used to measure cell viability and proliferation. Cells were seeded into 96-well plates (2×10^4 cells/well) and grown overnight, and then incubated with Fe_3O_4@PDA NPs at different concentrations (0, 25, 50, 75, 100, and 150 μg/mL). After 24-h incubation, CCK-8 reagent (Sigma-Aldrich)

was added to each well, and the cells were incubated for 2 h at 37 °C. The optimum density (OD) of cells in each well was measured at 450 nm (OD_{450}) using a microplate reader (Bio-Rad Laboratories Inc., Hercules, CA, USA).

Cells were incubated with 50 μg/mL nanoparticles for 24 h. Fe_3O_4@PDA NP-labeled cells were digested and seeded in 96-well plates (4×10^3/ well). At different time points (days 1, 3, 5 and 7), the CCK-8 reagent was added to measure the OD_{450} on a microplate reader to assess cell proliferation capacity.

2.8 Effects of Fe_3O_4@PDA NPs on UCMSC surface markers and differentiation

After incubation with Fe_3O_4@PDA NPs, the labeled and control cell populations (1×10^6) were washed three times with PBS and harvested. Then, cells were incubated with antibody cocktails against FITC CD90, PerCP-Cy™5.5 CD105, APC CD73, PE CD45, PE CD34, PE CD11b, PE CD19 and PE HLA-DR in the dark for 30 min at 4 °C. After incubation and two washing steps, the probe was measured using flow cytometry (FC500; Beckman Coulter Inc., Brea, CA, USA) with CXP software (Beckman Coulter Inc.). All antibodies were purchased from BD Biosciences.

To evaluate the osteogenic and adipogenic differentiation capacity of stem cells labeled with Fe_3O_4@PDA NPs, we performed differentiation induction experiments on labeled and unlabeled stem cells. UCMSCs were incubated with Fe_3O_4@PDA NPs (50 μg/mL) for 24 h, then the cells were digested and centrifuged. They were seeded into a 12-well plate (5×10^3 cells/cm^2). After 3 days of cell culture, different differentiation induction media were added. For the adipogenic induction, MSCs were grown in an adipogenic differentiation medium (StemPro Adipogenesis Differentiation Kit; Invitrogen Australia Pty Ltd; Australia). Cells were cultured for 14 days and the media were changed every 3 days. Then cells were stained with Oil Red O for further analysis of adipogenic differentiation. For the osteogenic induction, UCMSCs were grown in an osteogenic differentiation medium (StemPro Osteogenesis Differentiation Kit; Invitrogen Australia Pty Ltd; Australia). Cells were replaced with new medium every 3 days. After 21 days, cells were stained with 2% Alizarin Red S solution and visualized under a light microscope and images were captured for analysis.

2.9 Migration assays

The migratory ability of labeled and control UCMSCs was tested in a 24-well Transwell plate (FluoroBlok, 8.0 μm colored polyester membrane; BD Biosciences). Precisely, 1×10^6 cells in growth medium supplemented with 1% FBS were added to the top chambers and the lower chambers were filled with the growth medium containing 10% FBS. After incubating the plates for 24 h at 37 °C in a humidified 5% CO_2 atmosphere, cells on the lower side of the membranes were fixed with 4% paraformaldehyde for 15 min and counted under an optical microscope (X51; Olympus, Tokyo, Japan) after staining with 0.5% crystal violet (Sigma-Aldrich).

2.10 Animal experiments

The use of animals was approved by the Welfare and Research Ethics Committee on Animal Experiments of Jilin University. A total of 45 Sprague Dawley rats aged 6–8 weeks (nine rats/group) were used in this study. The IDD model was established by caudal needle puncture, as previously described.[36] Briefly, rats were anesthetized with 10% chloral hydrate (3.5 mL/kg) to identify and mark the six and seventh coccygeal vertebrae (Co6/Co7) via X-ray radiography (Faxitron X-ray, Lincolnshire, IL, USA) under appropriate parameters (35 kV, 300 mA and 1 min). A 22G needle was applied to percutaneously penetrate the IVD, rotated 360° and held in position for 30 s before extraction. Rats were subjected to standard postoperative procedures. Rats were randomly divided into 4 groups; control group, saline group, UCMSC group (MSC unlabeled with Fe_3O_4@PDA), and UCMSC + Fe_3O_4@PDA group (UCMSC labeled with Fe_3O_4@PDA). Twenty-four hours after surgery, cells (1×10^6) were resuspended in saline and then injected into the tail vein. Before injection, labeled and unlabeled UCMSCs were stained using CM-Dil (Sigma-Aldrich) according to manufacturer's instructions. All rats were euthanized after 2 weeks of treatment.

2.11 Calculation of disc height index (DHI)

Lateral plain radiographs of the rat tails were taken before and 2 weeks after injury using a cabinet X-ray system with an exposure time of 60 s and penetration power of 35 kV. The percentage of DHI was calculated using RadiAnt software as previously described.[37] The change in DHI was expressed as the %DHI [%DHI = (postpunctured DHI/prepunctured DHI) ×100]. Three independent observers independently measured and interpreted the radiographic images in a blinded manner.

2.12 Real-time quantitative polymerase chain reaction (RT-qPCR)

Total RNA was isolated from the cells of nucleus pulposus or Co6/7 using the Trizol reagent according to the manufacturer's instructions. RNA was reverse transcribed into cDNA according to the manufacturer's instructions. RT-qPCR was carried out using the ABI StepOnePlus RT-PCR System (Applied Biosystems, Foster City, CA, USA) with SYBR® Green PCR Master Mix (Applied Biosystems, Warrington, UK). The relative expressions of *aggrecan, type II collage*, *Sox-9*, *Mmp-13*, *Tnf-α*, and *Il-1β* were determined and normalized to the *GAPDH* housekeeping gene. The primers are presented in Table. 1. The real-time PCR thermo-cycler parameters consisted of an initial enzyme activation step at 95 °C for 10 min, followed by 40 cycles of 95 °C for 15 s, 55 °C for 15 s, and 72 °C for 30 s. The cycle threshold (Ct) value of each sample was calculated in triplicate. The $2^{-\Delta\Delta Ct}$ value was then used to calculate the target gene relative expression against *GAPDH* mRNA levels.[38]

2.13 Histological and immunohistochemical analysis of the IVD

Two weeks after cell transplantation, Co6/7 discs were harvested with adjacent vertebrae. Samples were fixed in 4% paraformaldehyde, decalcified in Morse's solution (22.5% formic acid, 10% sodium citrate in deionized water) and embedded in paraffin. Disks were sectioned at a thickness of 5 μm and then stained with Safranin-O-fast green as well as hematoxylin and eosin to analyze the histological grading score.[39]

The above sections were then used for immunohistochemistry to detect aggrecan, type II collagen, Sox-9, Mmp-13, Tnf-α and Il-1β. The sections were left at room temperature for 60 min and dewaxed twice with xylene (10 min each). Then, they were treated with 100, 95, 80, and 70% ethanol for 5 min, and washed three times with PBS. Endogenous peroxidase was inactivated with 3% hydrogen peroxide. Antigen retrieval was performed by heating the sample at 95 °C for 20 min in 10 mM sodium citrate (pH 6.0). Sections were incubated in 10% normal goat serum (Solarbio Company, Beijing, China) for 20 min to block non-specific binding. Then sections were l incubated overnight at 4 °C with the following primary antibodies: anti-aggrecan (1:100 dilution); anti-type II collagen (1:200 dilution); anti-SOX-9 (1:50); anti-Mmp-13 (1:200); anti-Tnf-α (1:200); anti-Il-1β (1:200) antibodies (Santa Cruz Biotech, Santa Cruz, CA, USA). The sections were washed with PBS and incubated with the corresponding secondary antibody for 2 h at room temperature. Cell nuclei were stained by 4, 6'-diamino-2-phenylindole (DAPI, HARVEY, USA). The sections were observed using an optical microscope (Olympus, Tokyo, Japan).

2.14 Evaluation migration of transplanted UCMSCs

We used immunofluorescence technology to study the fate of CM-Dil-labeled UCMSCs after transplantation. Two weeks after cell transplantation, Co6/7 discs were harvested, fixed and decalcified with adjacent vertebrae. The intervertebral disc tissue was sliced into 5-μm sections by a freezing microtome (LEICA, Germany). The nuclei were stained with 4', 6'-diamino-2-phenylindole (DAPI, HARVEY, USA). Sections were observed using a fluorescence microscope (Olympus Corporation, Tokyo, Japan) to analyze the positive of CM-Dil-labeled cells.

2.15 Statistical analysis

SPSS version 22.0 software (Chicago, Illinois, USA) was used for statistical analysis. ANOVA was used for statistical analysis. Statistical significance was defined as P□0.05.

3. Results

3.1 Characterization of Fe_3O_4@PDA NPs

In the current study, water-dispersible, uniformly distributed PDA-coated Fe_3O_4 NPs were synthesized. TEM images showed that the prepared Fe_3O_4 NPs was very uniformly dispersed (Fig. 1B), and we observed an average particle size of about 50 nm. The average diamBeter was about 53.50 nm (Fig. 1C).

3.2 Internalization of Fe_3O_4@PDA NPs

To study the cellular uptake of Fe_3O_4@PDA NPs, we used ICP-OES and quantified iron in cell lysates after a 24-h co-incubation. ICP-OES results revealed that Fe_3O_4@PDA NPs were taken up by UCMSCs in a dose-dependent manner (Fig. 2A). Furthermore, we used TEM to further observe the fate of the particles after being phagocytosed by the cells, and the results showed that the particles mainly existed in the cytoplasm (Fig. 2B). To observe the internalization more directly and labeling efficiency of Fe3O4@PDA

NPs, Prussian blue staining was used. The results were consistent with ICP-OES measurements; after the higher dose treatment, more NPs were internalized by the cells (Fig. 2C). When the NP concentration was not less than 50 μg/mL, the cells could be effectively labeled.

3.3 Biocompatibility of Fe_3O_4@PDA NPs

Fe_3O_4@PDA NP-labeled UCMSCs for stem cell treatment depended largely on the effects of NPs on the survival and proliferation of UCMSCs. We studied the viability and proliferation of Fe_3O_4@PDA NP-labeled UCMSCs. To evaluate the toxicity of Fe_3O_4@PDA NPs, we incubated UCMSCs with various concentrations of Fe_3O_4@PDA NPs for 24 h and then performed CCK-8 to determine cell viability. Over 93% of MSCs were still viable at Fe_3O_4@PDA NP concentrations of 0, 25, 50, 75, 100,150 and 200 μg/mL (Fig. 2D). There was no statistical significance among different concentrations. At the NP concentration of 50 μg/mL, the cell viability was not affected and the cells could effectively be labeled; therefore, we chose 50 μg/mL Fe_3O_4@PDA NP concentration for further experiments. To assess the potential influence of NPs on UCMSC proliferation, we evaluated cell proliferation (1, 3, 5 and 7 days) after the stem cells were labeled with Fe_3O_4@PDA NPs. Compared with the control, NP-labeled UCMSCs showed similar proliferation rates without statistical significance (Fig. 2E).

3.4 Impact of Fe_3O_4@PDA NPs on UCMSC functionality

To determine whether Fe3O4@PDA NP labeling changed stem cell characteristics in UCMSCs, we used flow cytometry and analyzed the expression of characteristic markers on the surface of unlabeled and labeled stem cells. NP labeling did not alter the expression of typical surface markers on UCMSCs (Fig. 3A). In addition, NP-labeled and unlabeled UCMSCs were cultured in osteogenic and adipogenic differentiation media to evaluate the effect of NP labeling on stem cell differentiation. As shown in Fig. 3B, unlabeled and labeled cells had good osteogenic and adipogenic differentiation abilities.

3.5 Enhanced migration capacity of Fe_3O_4@PDA NP-labeled MSCs in vitro

Transwell experiments showed that nanoparticle labeling enhanced the migration of UCMSCs. There were significantly more migrated cells in the NP-labeled stem cell group than in the unlabeled group (Fig. 4A-B). We examined the mRNA and protein expression to study whether NPs increased UCMSC migration via CXCR4. As shown in Fig. 4C-D, the gene and protein expression levels of CXCR4 in the labeled group were higher than unlabeled group.

3.6 IVD height radiographic changes and histological evaluation

Radiographs were taken for each disc before and 2 weeks after the puncture. The %DHI remained relatively stable in the control group whereas it decreased continuously in all three operated groups (saline, unlabeled UCMSC, and labeled UCMSC groups). The %DHI of the saline and unlabeled UCMSC groups continued to decrease during the entire experimental period. The %DHI of the labeled UCMSC group was higher than that of the saline and unlabeled UCMSC groups ($P < 0.01$) (Fig. 5A-B).

To quantify the degree of disc degeneration, we used a histological grading scale to assess the number and morphology of annulus fibrosus AF cells, the boundary between AF and nucleus pulposus, and the number and morphology of nucleus pulposus cells. As shown in Fig. 5C-D, H&E and Safranin-O/fast green staining revealed that the annulus fibrosus was composed of regularly arranged slices and NP appeared as an organized structure with abundant cellular components in the control group. In the saline group, the nucleus pulposus tissue had completely disappeared and the annulus fibrosus structures were destroyed. The groups treated with unlabeled and labeled UCMSCs improved the regeneration of nucleus pulposus and annulus fibrosus, whereas Safranin-O staining of the nucleus pulposus tissue was deeper and that of the AF tissue structure was more complete in the labeled UCMSCs group.

3.7 Fe_3O_4@PDA NP labeling enhanced UCMSC migration in degenerated IVD

To track cell migration into the coccygeal IVDs in rats in vivo, CM-Dil-labeled UCMSCs were detected in IVD after 2 weeks of cell transplantation. A large number of systemic injections of Dil-labeled UCMSCs were observed around the IVD, but fewer cells appeared at the center of the IVD. As shown in Fig. 6A, the number of labeled UCMSCs entering the disc increased. These results meant that much more UCMSCs in the labeled group can migrated into IVD than in the unlabeled group, and Fe_3O_4@PDA NPs upregulated enhanced the migration ability of UCMSCs to homing into degenerated IVD.

3.8 Gene expression and immunohistochemical analysis

To confirm the effect of UCMSCs transplantation on the disc matrix, the expression of *acan*, *Col 2*, *Sox-9*, *Mmp-13*, *Tnf-α*, and *Il-1β* in the disc were measured using real-time PCR. Two weeks after injury, the mRNA expression of *acan*, *Col 2*, and *Sox-9* was decreased in the saline, unlabeled UCMSC, and labeled UCMSC groups compared with the control group, while *Mmp-13*, *Tnf-α*, and *Il-1β* expression was significantly increased in the saline, unlabeled UCMSC, and labeled UCMSC groups. Compared with the unlabeled UCMSC group, the expression of *acan*, *Col 2*, and *Sox-9* mRNAs in the labeled UCMSC group was significantly increased, while that of *Mmp-13*, *Tnf-α*, and *Il-1β* was significantly decreased (Fig. 6B). The results showed that the labeled stem cells had increased aggrecan, type 2 collagen and Sox-9, and reduced Mmp-13, Tnf-α, and Il-1β expression.

Figure 6C showed the immunohistochemical analysis of the expression of aggrecan, type 2 collagen, Sox-9, Mmp-13, Tnf-α and Il-1β in the nucleus pulposus tissue in different groups. Compared with the control group, aggrecan, type 2 collagen and Sox-9 expressions significantly decreased in the saline,

unlabeled UCMSC, and labeled UCMSC groups. Mmp-13, Tnf-α and Il-1β expressions significantly increased in the saline, unlabeled UCMSC, and labeled UCMSC groups compared with the contol group. Aggrecan, type 2 collagen, and Sox-9 expressions were significantly higher in the labeled group than in the unlabeled group. In comparison with the unlabeled group, the Mmp-13, Tnf-α and Il-1β expression decreased drastically in the labeled group.

3.9 In vivo toxicity Test

Exactly 14 days after treatment, H&E staining was performed on the heart, liver, spleen, lung, and kidney of each group to analyze the toxicity of NPs to rats. H&E staining histological analysis did not reveal any morphological changes in the heart, liver, spleen, lungs, or kidneys in each group, further confirming the low toxicity of Fe_3O_4@PDA NPs in vivo (Fig. 7).

4. Discussion

The purpose of this study was to prove the hypothesis that nanoparticles enhance the ability of UCMSCs to repair IDD by increasing the migration of implanted cells. We have demonstrated the efficiency and safety of Fe_3O_4@PDA NP-labeled UCMSCs, which increased stem cell migration in vitro and effectively repaired degenerated discs in a rat caudal disc degeneration model after systemic injection.

MSC transplantation for the treatment of IDD has been recognized as a promising strategy. [40] One of the main obstacles of cell therapy to treat IVD degeneration is the method of delivery, which is largely limited to direct injection into IVD due to its avascular nature.[41] Whether the regeneration potential of stem cells in degenerated IVD tissue is due to the transdifferentiation and replacement of dead cells, or due to the secretion of soluble factors to stimulate local progenitor cell survival, proliferation, and differentiation is still a subject of debate.[42] Increasing evidence shows that the efficiency of MSC homing to injured tissues is an important parameter that affects the outcome of MSC treatment. Although the exact molecular mechanism by which MSCs migrate and enter the injury site is not fully understood, pretreatment of MSCs with genetic modification, specific cytokines, or hypoxia to overexpress CXCR4 can promote the migration of MSCs to damaged tissues.[43] Therefore, using the homing ability of stem cells may bypass the risks associated with direct injection.

The characteristic of Fe_3O_4@PDA NPs in enhancing the expression of CXCR4 in stem cells will undoubtedly expand the application of them in nanomedicine. Unlike the complex process and potential safety concerns of altering the cell surface through conjugation of specific proteins and retroviral vectors encoding homing receptors, this simple method was implemented by adding the appropriate concentration of Fe_3O_4@PDA NPs to the medium. After being internalized by the cell, Fe_3O_4@PDA NPs may be degraded into iron ions in the lysosome by hydrolytic enzymes.[44] After entering the mitochondrial membrane, iron ions can react with hydrogen peroxide and oxygen produced by mitochondria. Apopa et al. reported that reactive oxygen species (ROS) produced by iron NPs increase human microvascular endothelial cell permeability.[45] Yun et al. found that CXCR4 expression in MSCs is increased by

internalizing Fe_3O_4 NPs into cells and the level of ROS in MSCs also is increased accordingly. CXCR4 expression and the ROS level can be induced by Fe_3O_4 NPs in a time- and concentration-dependent manner.[46] Xu et al. showed that the migration of MSCs via the up-regulation of CXCR4 is induced by iron-containing NPs, and iron-containing NP-loaded MSCs with high CXCR4 expression maintain good biological activity and can migrate to cancer cells in vivo and in vitro.[47] Other studies have shown that iron overload can lead to harmful cellular consequences and enhanced cell proliferation by changing the expressions of genes involved in cell cycle control and reducing intracellular hydrogen peroxide.[48] Therefore, the choice of NP concentration is also very important for the migration of cells. Consistent with these studies, 50 μg/mL of Fe_3O_4@PDA NPs increased the migration of stem cells in this study. These results indicated that the regulation of CXCR4 by Fe_3O_4@PDA NPs might be a complex process involving various mechanisms in different cellular environments. The detailed mechanism will be further explored in future research.

Although the special microenvironment without blood vessels in inner AF and NP leads us to speculate that MSCs will not migrate into IVD, recent research suggested that MSCs can be recruited to respond to IVD lesions.[40] Illien-Jünger et al. demonstrated that degenerative conditions induce the release of factors promoting MSC recruitment in an ex vivo organ culture.[49] Zhang et al. prepared nanomaterials for a sustained release of stromal cell-derived factor-1α (SDF-1α), to recruit MSCs and in turn achieve regeneration of IVD.[50] Sakai et al found that during degeneration of the IVD, cells from the bone marrow can migrate to the IVD. The frequency of the cells is related to the blood vessel distribution of the IVD. As the distance from the blood vessel increases, fewer cells appear, and the migration effect becomes limited.[51] SDF-1α, also known as CXC motif chemokine 12 (CXCL12), is a powerful chemokine cytokine that plays a key role in the recruitment, proliferation and differentiation of stem cells. CXCR4 is a specific receptor for SDF-1, which is widely expressed on stem cells.[52] SDF-1α are reportedly upregulated during the degeneration of IVD.[53] CXCR4 overexpression promotes MSC retention within the IVD and enhances the stem cell-based IVD regeneration.[54] Consistently, our results showed that labeling UCMSCs with Fe_3O_4@PDA NPs increased stem cell CXCR4 expression and effectively repaired degenerated discs. In addition to homing to the lesion, MSCs also participate in the repair process through their paracrine function. MSCs produce large amounts of growth factors, and communication with the inflammatory microenvironment is an important part of this process.[55] It has been demonstrated that the expression of proinflammatory mediators, TNF-α and IL-1β, increase in the degenerated disc tissue.[56] Some reports have shown that the immunomodulatory and anti-inflammatory effects of MSCs may help modulate the IVD repair process.[57]

In the present study, we found that UCMSCs labeled with Fe_3O_4@PDA NPs decreased the expression of Mmp-13, Tnf-α and Il-1β and promoted the expression of aggrecan, type 2 collagen, and Sox-9 in the degenerated disc tissue of rats. These findings might suggest that the SDF-1/CXCR4 axis played an important role in mediating MSC homing to IDD and paracrine function of MSCs might contribute to facilitating IDD regeneration. Our results showed UCMSCs labeled with Fe_3O_4@PDA NPs increased

homing ability and could be transported through the tail vein of rats to the IVD, where there was a physical barrier and had the additional advantage of repeated treatment when necessary. However, the environment and degenerate model of IVD is different between rats and humans. Further transplantation studies should be performed using UCMSCs labeled with Fe_3O_4@PDA NPs in clinical applications.

The timing of cell therapy for disc degeneration is controversial. During disc degeneration, homeostasis gradually becomes disturbed and eventually leads to a pathological condition. Some studies suggested that the best time to treat disc degeneration is 2 or 4 weeks after disc injury and they concluded that the therapeutic effect of MSCs injection is more optimal in a later stage of degeneration rather than in early stages.[58] Other studies reported that for cell therapy, immediately or 24 hours after disc injury is the best time to treat disc degeneration and they postulated that a narrow window of opportunity may exist for a maximum therapeutic effect during the early stages of degeneration.[59] Within the scope of this study, we did not use magnetic resonance imaging to track the fate of stem cells labeled with Fe_3O_4@PDA NPs, because Fe_3O_4 NPs are negative contrast agents and affect our evaluation of disc.[60]

5. Conclusions

In conclusion, systemic transplantation of UCMSCs labeled with Fe_3O_4@PDA NPs retards IDD via enhancing migration and decreasing proinflammatory mediators in rats, which provides an efficient way to improve the effects of UCMSC transplantation in IDD treatment.

Declarations

Acknowledgements

Not applicable.

Author Contributions

Conceptualization, Meng Zhang and Butain Zhang; methodology, Meng Zhang; software, Ran Li; validation, Meng Zhang and Te Liu.; formal analysis, Jun Zhang; investigation, Ying Wang; data curation, Xupeng Mu; writing—original draft preparation, Meng Zhang; writing—review and editing, Jinlan Jiang; visualization, Fuqiang Zhang; supervision, Jinlan Jiang; project administration, Xupeng Mu. All authors have read and agreed to the published version of the manuscript.

Consent for publication

Not applicable.

Funding

This study was financially supported by the Science and Technology Development Plan Projects of Jilin Province (Grant No. 20200201558JC). This work was supported by the National Natural Science

Foundation of China (Grant No. 81903273), the Jilin Province Science and Technology Development Plan Project (Grant No. 20200201429JC, 20190103078JH, 20190304030YY, 20190902007TC, 20190908002TC and 20190901007JC), the Health Special Project of Jilin Provincial Finance Department (Grant No. 2019SCZ059 and 2018scz034) and the Project of Jilin development and Reform Commission (2019C016).

Availability of data and materials

Not applicable.

Ethics approval and consent to participate

This study was approval by the Ethic Committee at Jilin university. The use of animals for research purposes was in accordance with the Declaration of Helsinki, and the research did not contain any individual person's data in any form.

Conflicts of Interest: The authors declare no conflict of interest.

Authors' information

Meng Zhang, email addresses: 645135899@qq.com

Butian Zhang, email addresses: zhangbt@jlu.edu.cn

Ran Li, email addresses: rany@jlu.edu.cn

Te Liu, email addresses: liute@jlu.edu.cn

Jun Zhang, email addresses: 947978224@qq.com

Ying Wang, email addresses: 378953757@qq.com

Fuqiang Zhang, email addresses: zfqzhang@jlu.edu.cn

Xupeng Mu, email addresses: muxupeng@jlu.edu.cn

Jinlan Jiang, email addresses: jiangjinlan@jlu.edu.cn

References

[1] Kepler CK, Ponnappan RK, Tannoury CA, Risbud MV, Anderson DG. The molecular basis of intervertebral disc degeneration. The spine journal : official journal of the North American Spine Society 2013;13:318-30. DOI: 10.1016/j.spinee.2012.12.003.

[2] Sakai D, Grad S. Advancing the cellular and molecular therapy for intervertebral disc disease. Advanced drug delivery reviews 2015;84:159-71. DOI: 10.1016/j.addr.2014.06.009.

[3] Hurwitz EL, Randhawa K, Yu H, Côté P, Haldeman S. The Global Spine Care Initiative: a summary of the global burden of low back and neck pain studies. Eur Spine J. 2018;27:796-801. DOI: 10.1007/s00586-017-5432-9.

[4] Fontana G, See E, Pandit A. Current trends in biologics delivery to restore intervertebral disc anabolism. Advanced drug delivery reviews 2015;84:146-58. DOI: 10.1016/j.addr.2014.08.008.

[5] Blanquer SBG, Grijpma DW, Poot AA. Delivery systems for the treatment of degenerated intervertebral discs. Advanced drug delivery reviews 2015;84:172-87. Doi: 10.1016/j.addr.2014.10.024.

[6] Wang W, Wang Y, Deng G, Ma J, Huang X, Yu J, et al. Transplantation of Hypoxic-Preconditioned Bone Mesenchymal Stem Cells Retards Intervertebral Disc Degeneration via Enhancing Implanted Cell Survival and Migration in Rats. Stem cells international 2018;2018:7564159. DOI: 10.1155/2018/7564159.

[7] Sakai D, Andersson GBJ. Stem cell therapy for intervertebral disc regeneration: obstacles and solutions. Nature reviews Rheumatology 2015;11:243-56. DOI: 10.1038/nrrheum.2015.13.

[8] Arkesteijn ITM, Smolders LA, Spillekom S, Riemers FM, Potier E, Meij BP, et al. Effect of coculturing canine notochordal, nucleus pulposus and mesenchymal stromal cells for intervertebral disc regeneration. Arthritis research & therapy 2015;17:60. DOI: 10.1186/s13075-015-0569-6.

[9] Daly CD, Ghosh P, Zannettino ACW, Badal T, Shimmon R, Jenkin G, et al. Mesenchymal progenitor cells primed with pentosan polysulfate promote lumbar intervertebral disc regeneration in an ovine model of microdiscectomy. Spine J. 2018 Mar;18(3):491-506. DOI: 10.1016/j.spinee.2017.10.008.

[10] Ding DC, Chang YH, Shyu WC, Lin SZ. Human umbilical cord mesenchymal stem cells: a new era for stem cell therapy. Cell transplantation 2015;24:339-47. DOI: 10.3727/096368915X686841.

[11] Davies JE, Walker JT, Keating A. Concise Review: Wharton's Jelly: The Rich, but Enigmatic, Source of Mesenchymal Stromal Cells. Stem cells translational medicine 2017;6:1620-30. DOI: 10.1002/sctm.16-0492.

[12] Scheers I, Lombard C, Paganelli M, Campard D, Najimi M, Gala JL, et al. Human umbilical cord matrix stem cells maintain multilineage differentiation abilities and do not transform during long-term culture. PloS one 2013;8:e71374. DOI: 10.1371/journal.pone.0093726.

[13] Martin JT, Gorth DJ, Beattie EE, Harfe BD, Smith LJ, Elliott DM. Needle puncture injury causes acute and long-term mechanical deficiency in a mouse model of intervertebral disc degeneration. Journal of orthopaedic research : official publication of the Orthopaedic Research Society 2013;31:1276-82. DOI: 10.1002/jor.22355.

[14] Yang F, Leung VYL, Luk KDK, Chan D, Cheung KMC. Mesenchymal stem cells arrest intervertebral disc degeneration through chondrocytic differentiation and stimulation of endogenous cells. Molecular

therapy : the journal of the American Society of Gene Therapy 2009;17:1959-66. DOI: 10.1038/mt.2009.146.

[15] Grunhagen T, Wilde G, Soukane DM, Shirazi-Adl SA, Urban JPG. Nutrient supply and intervertebral disc metabolism. The Journal of bone and joint surgery American volume 2006;88 Suppl 2:30-5. DOI: 10.2106/JBJS.E.01290.

[16] Li YY, Diao HJ, Chik TK, Chow CT, An XM, Leung V, et al. Delivering mesenchymal stem cells in collagen microsphere carriers to rabbit degenerative disc: reduced risk of osteophyte formation. Tissue engineering Part A 2014;20:1379-91. DOI: 10.1089/ten.TEA.2013.0498.

[17] Yu Q, Liu L, Lin J, Wang Y, Xuan X, Guo Y, et al. SDF-1α/CXCR4 Axis Mediates The Migration of Mesenchymal Stem Cells to The Hypoxic-Ischemic Brain Lesion in A Rat Model. Cell J 2015;16:440-7. DOI: 10.22074/cellj.2015.504.

[18] Illien-Jünger S, Pattappa G, Peroglio M, Benneker LM, Stoddart MJ, Sakai D, et al. Homing of mesenchymal stem cells in induced degenerative intervertebral discs in a whole organ culture system. Spine 2012;37:1865-73. DOI: 10.1097/BRS.0b013e3182544a8a.

[19] Tam V, Rogers I, Chan D, Leung VYL, Cheung KMC. A comparison of intravenous and intradiscal delivery of multipotential stem cells on the healing of injured intervertebral disk. Journal of orthopaedic research : official publication of the Orthopaedic Research Society 2014;32:819-25. DOI: 10.1002/jor.22605.

[20] Sakai D, Nishimura K, Tanaka M, Nakajima D, Grad S, Alini M, et al. Migration of bone marrow-derived cells for endogenous repair in a new tail-looping disc degeneration model in the mouse: a pilot study. The spine journal : official journal of the North American Spine Society 2015;15:1356-65. DOI: 10.1016/j.spinee.2013.07.491.

[21] Cunha C, Almeida CR, Almeida MI, Silva AM, Molinos M, Lamas S, et al. Systemic Delivery of Bone Marrow Mesenchymal Stem Cells for In Situ Intervertebral Disc Regeneration. Stem cells translational medicine 2017;6:1029-39. DOI: 10.5966/sctm.2016-0033.

[22] Sohni A, Verfaillie CM. Mesenchymal stem cells migration homing and tracking. Stem cells international 2013;2013:130763. DOI: 10.1155/2013/130763.

[23] Walter DH, Haendeler J, Reinhold J, Rochwalsky U, Seeger F, Honold J, et al. Impaired CXCR4 signaling contributes to the reduced neovascularization capacity of endothelial progenitor cells from patients with coronary artery disease. Circ Res 2005;97:1142-51. DOI: 10.1161/01.RES.0000193596.94936.2c.

[24] Belema-Bedada F, Uchida S, Martire A, Kostin S, Braun T. Efficient homing of multipotent adult mesenchymal stem cells depends on FROUNT-mediated clustering of CCR2. Cell stem cell 2008;2:566-75.

DOI: 10.1016/j.stem.2008.03.003.

[25] Wynn RF, Hart CA, Corradi-Perini C, O'Neill L, Evans CA, Wraith JE, et al. A small proportion of mesenchymal stem cells strongly expresses functionally active CXCR4 receptor capable of promoting migration to bone marrow. Blood 2004;104:2643-5. DOI: 10.1182/blood-2004-02-0526

[26] De Becker A, Riet IV. Homing and migration of mesenchymal stromal cells: How to improve the efficacy of cell therapy? World J Stem Cells 2016;8:73-87. DOI: 10.4252/wjsc.v8.i3.73

[27] Yoo J-W, Irvine DJ, Discher DE, Mitragotri S. Bio-inspired, bioengineered and biomimetic drug delivery carriers. Nat Rev Drug Discov 2011;10:521-35. DOI: 10.1038/nrd3499

[28] Mu X, Zhang F, Kong C, Zhang H, Zhang W, Ge R, et al. EGFR-targeted delivery of DOX-loaded FeO@ polydopamine multifunctional nanocomposites for MRI and antitumor chemo-photothermal therapy. International journal of nanomedicine 2017;12:2899-911. DOI: 10.2147/IJN.S131418

[29] Gu L, Li X, Jiang J, Guo G, Wu H, Wu M, et al. Stem cell tracking using effective self-assembled peptide-modified superparamagnetic nanoparticles. Nanoscale 2018;10:15967-79. DOI: 10.1039/c7nr07618e

[30] Meng Y, Shi C, Hu B, Gong J, Zhong X, Lin X, et al. External magnetic field promotes homing of magnetized stem cells following subcutaneous injection. BMC Cell Biol 2017;18:24. DOI: 10.1186/s12860-017-0140-1

[31] Li X, Wei Z, Lv H, Wu L, Cui Y, Yao H, et al. Iron oxide nanoparticles promote the migration of mesenchymal stem cells to injury sites. International journal of nanomedicine 2019;14:573-89. DOI: 10.2147/IJN.S184920

[32] Huang X, Zhang F, Wang Y, Sun X, Choi KY, Liu D, et al. Design considerations of iron-based nanoclusters for noninvasive tracking of mesenchymal stem cell homing. ACS nano 2014;8:4403-14. DOI: 10.1021/nn4062726

[33] Ahn YJ, Kong TH, Choi JS, Yun WS, Key J, Seo YJ. Strategies to enhance efficacy of SPION-labeled stem cell homing by magnetic attraction: a systemic review with meta-analysis. International journal of nanomedicine 2019;14:4849-66. DOI: 10.2147/IJN.S204910

[34] Li X, Wei Z, Li B, Li J, Lv H, Wu L, et al. In vivo migration of FeO@polydopamine nanoparticle-labeled mesenchymal stem cells to burn injury sites and their therapeutic effects in a rat model. Biomaterials science 2019;7:2861-72. DOI: 10.1039/c9bm00242a

[35] Sun S, Zeng H. Size-controlled synthesis of magnetite nanoparticles. J Am Chem Soc 2002;124:8204-5. DOI: 10.1021/ja026501x

[36] Han B, Zhu K, Li F-C, Xiao Y-X, Feng J, Shi Z-L, et al. A simple disc degeneration model induced by percutaneous needle puncture in the rat tail. Spine 2008;33:1925-34. DOI: 10.1097/BRS.0b013e31817c64a9

[37] MacLean JJ, Lee CR, Alini M, Iatridis JC. The effects of short-term load duration on anabolic and catabolic gene expression in the rat tail intervertebral disc. Journal of orthopaedic research : official publication of the Orthopaedic Research Society 2005;23:1120-7. DOI: 10.1016/j.orthres.2005.01.020

[38] Livak KJ, Schmittgen TD. Analysis of relative gene expression data using real-time quantitative PCR and the 2(-Delta Delta C(T)) Method. Methods (San Diego, Calif) 2001;25:402-8. DOI: 10.1006/meth.2001.1262

[39] Rousseau M-AA, Ulrich JA, Bass EC, Rodriguez AG, Liu JJ, Lotz JC. Stab incision for inducing intervertebral disc degeneration in the rat. Spine 2007;32:17-24. DOI: 10.1097/01.brs.0000251013.07656.45

[40] Clouet J, Fusellier M, Camus A, Le Visage C, Guicheux J. Intervertebral disc regeneration: From cell therapy to the development of novel bioinspired endogenous repair strategies. Adv Drug Deliv Rev 2019;146:306-24. DOI: 10.1016/j.addr.2018.04.017 DOI: 10.1016/j.addr.2018.04.017

[41] Fontana G, See E, Pandit A. Current trends in biologics delivery to restore intervertebral disc anabolism. Adv Drug Deliv Rev 2015;84:146-58. DOI: 10.1016/j.addr.2014.08.008

[42] Yim RL, Lee JT, Bow CH, Meij B, Leung V, Cheung KM, et al. A systematic review of the safety and efficacy of mesenchymal stem cells for disc degeneration: insights and future directions for regenerative therapeutics. Stem Cells Dev 2014;23:2553-67. DOI: 10.1089/scd.2014.0203 DOI: 10.1089/scd.2014.0203

[43] Wang W, Wang Y, Deng G, Ma J, Huang X, Yu J, et al. Transplantation of Hypoxic-Preconditioned Bone Mesenchymal Stem Cells Retards Intervertebral Disc Degeneration via Enhancing Implanted Cell Survival and Migration in Rats. Stem cells international 2018;2018:7564159. DOI: 10.1155/2018/7564159

[44] Landázuri N, Tong S, Suo J, Joseph G, Weiss D, Sutcliffe DJ, et al. Magnetic targeting of human mesenchymal stem cells with internalized superparamagnetic iron oxide nanoparticles. Small (Weinheim an der Bergstrasse, Germany) 2013;9:4017-26. DOI: 10.1002/smll.201300570

[45] Apopa PL, Qian Y, Shao R, Guo NL, Schwegler-Berry D, Pacurari M, et al. Iron oxide nanoparticles induce human microvascular endothelial cell permeability through reactive oxygen species production and microtubule remodeling. Particle and fibre toxicology 2009;6:1. DOI: 10.1186/1743-8977-6-1

[46] Yun WS, Choi JS, Ju HM, Kim MH, Choi SJ, Oh ES, et al. Enhanced Homing Technique of Mesenchymal Stem Cells Using Iron Oxide Nanoparticles by Magnetic Attraction in Olfactory-Injured

Mouse Models. International journal of molecular sciences 2018;19. DOI: 10.3390/ijms19051376

[47] Xu C, Feng Q, Yang H, Wang G, Huang L, Bai Q, et al. A Light-Triggered Mesenchymal Stem Cell Delivery System for Photoacoustic Imaging and Chemo-Photothermal Therapy of Triple Negative Breast Cancer. Advanced science (Weinheim, Baden-Wurttemberg, Germany) 2018;5:1800382. DOI: 10.1002/advs.201800382

[48] Huang DM, Hsiao JK, Chen YC, Chien LY, Yao M, Chen YK, et al. The promotion of human mesenchymal stem cell proliferation by superparamagnetic iron oxide nanoparticles. Biomaterials 2009;30:3645-51. DOI: 10.1016/j.biomaterials.2009.03.032

[49] Illien-Jünger S, Pattappa G, Peroglio M, Benneker LM, Stoddart MJ, Sakai D, et al. Homing of mesenchymal stem cells in induced degenerative intervertebral discs in a whole organ culture system. Spine 2012;37:1865-73. DOI: 10.1097/BRS.0b013e3182544a8a

[50] Zhang H, Yu S, Zhao X, Mao Z, Gao C. Stromal cell-derived factor-1α-encapsulated albumin/heparin nanoparticles for induced stem cell migration and intervertebral disc regeneration in vivo. Acta biomaterialia 2018;72:217-27. DOI: 10.1016/j.actbio.2018.03.032

[51] Sakai D, Nishimura K, Tanaka M, Nakajima D, Grad S, Alini M, et al. Migration of bone marrow-derived cells for endogenous repair in a new tail-looping disc degeneration model in the mouse: a pilot study. The spine journal : official journal of the North American Spine Society 2015;15:1356-65. DOI: 10.1016/j.spinee.2013.07.491

[52] Lapidot T, Kollet O. The essential roles of the chemokine SDF-1 and its receptor CXCR4 in human stem cell homing and repopulation of transplanted immune-deficient NOD/SCID and NOD/SCID/B2m(null) mice. Leukemia 2002;16:1992-2003. DOI: 10.1038/sj.leu.2402684

[53] Jia CQ, Zhao JG, Zhang SF, Qi F. Stromal cell-derived factor-1 and vascular endothelial growth factor may play an important role in the process of neovascularization of herniated intervertebral discs. The Journal of international medical research 2009;37:136-44. DOI: 10.1177/147323000903700116

[54] Wei JN, Cai F, Wang F, Wu XT, Liu L, Hong X, et al. Transplantation of CXCR4 Overexpressed Mesenchymal Stem Cells Augments Regeneration in Degenerated Intervertebral Discs. DNA and cell biology 2016;35:241-8. DOI: 10.1089/dna.2015.3118

[55] Strassburg S, Hodson NW, Hill PI, Richardson SM, Hoyland JA. Bi-directional exchange of membrane components occurs during co-culture of mesenchymal stem cells and nucleus pulposus cells. PloS one 2012;7:e33739. DOI: 10.1371/journal.pone.0033739

[56] Risbud MV, Shapiro IM. Role of cytokines in intervertebral disc degeneration: pain and disc content. Nature reviews Rheumatology 2014;10:44-56. DOI: 10.1038/nrrheum.2013.160

[57] Sakai D, Andersson GB. Stem cell therapy for intervertebral disc regeneration: obstacles and solutions. Nature reviews Rheumatology 2015;11:243-56. DOI: 10.1038/nrrheum.2013.160

[58] Zhang Y, Tao H, Gu T, Zhou M, Jia Z, Jiang G, et al. The effects of human Wharton's jelly cell transplantation on the intervertebral disc in a canine disc degeneration model. Stem cell research & therapy 2015;6:154. DOI: 10.1186/s13287-015-0132-z

[59] Ishiguro H, Kaito T, Yarimitsu S, Hashimoto K, Okada R, Kushioka J, et al. Intervertebral disc regeneration with an adipose mesenchymal stem cell-derived tissue-engineered construct in a rat nucleotomy model. Acta biomaterialia 2019;87:118-29. DOI: 10.1016/j.actbio.2019.01.050

[60] Riegler J, Liew A, Hynes SO, Ortega D, O'Brien T, Day RM, et al. Superparamagnetic iron oxide nanoparticle targeting of MSCs in vascular injury. Biomaterials 2013;34:1987-94. DOI: 10.1016/j.biomaterials.2012.11.040

Tables

Table 1 Primer sequences and product sizes

Symbol	Primer Sequence	Product Size (bp)
GAPDH	F-CTGGAGAAACCTGCCAAGTATG	138
	R-GGTGGAAGAATGGGAGTTGCT	
Aggrecan,	F-CTGGGCGTGAGGACCGTCTAC	293
	R-GTGTAGCAGATGGCGTCGTAGC	
Type II collage	F-ACCATATCGCTCAAAAGGAAGGTCTG	128
	R-AGCTGGTCTCTTCTCTTGGTCTCC	
Sox-9	F-CACACGCTGACCACGCTGAG	158
	R-GCTGCTGCTGCTCGCTGTAG	
Mmp-13	F-GCCACCTTCTTCTTGTTGAGTTG	161
	R-GACTTCTTCAGGATTCCCGCA	
Tnf-α	F-TCATCTACTCCCAGGTCCTCTTCAAG	172
	R-GACGGCGATGCGGCTGATG	
Il-1β	F-GAACAACAAAAATGCCTCGTGC	264
	R-GACAAACCGCTTTTCCATCTTCT	
CXCR4	F-TCCTGCCCACCATCTACTCCATC	193
	R-CCTGTACTTGTCCGTCATGCTTCTC	

Figures

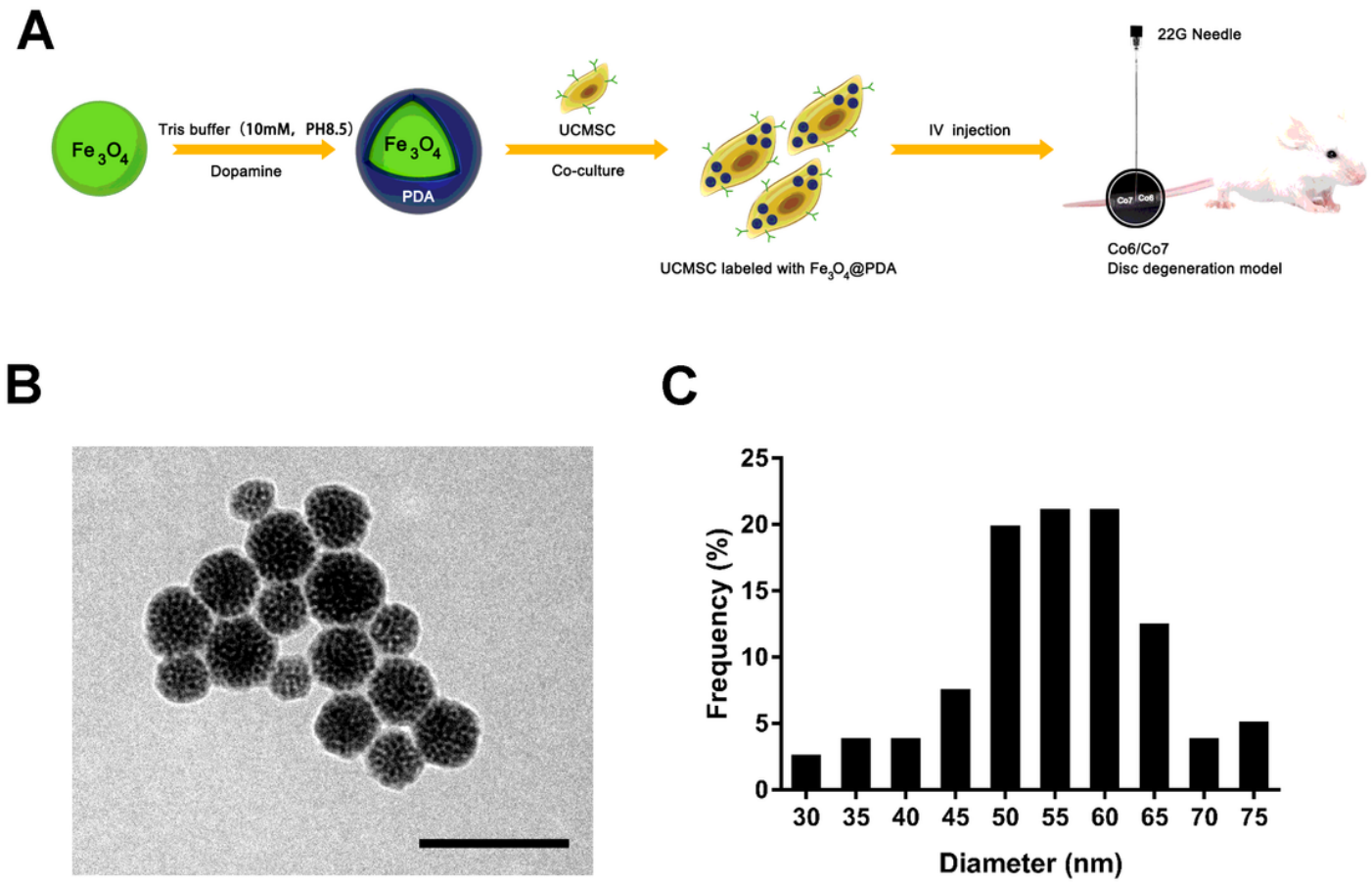

Figure 1

(A) Schematic illustration systemic delivery of UCMSCs labeled with Fe3O4@PDA NPs improved the therapeutic efficacy in a disc degeneration rat model via enhancing migration and decreasing proinflammatory mediators. (B) Transmission electron microscopy of Fe3O4@PDA NPs. Scale bar = 50 μm. (C) Size distribution of Fe3O4@PDA NPs.

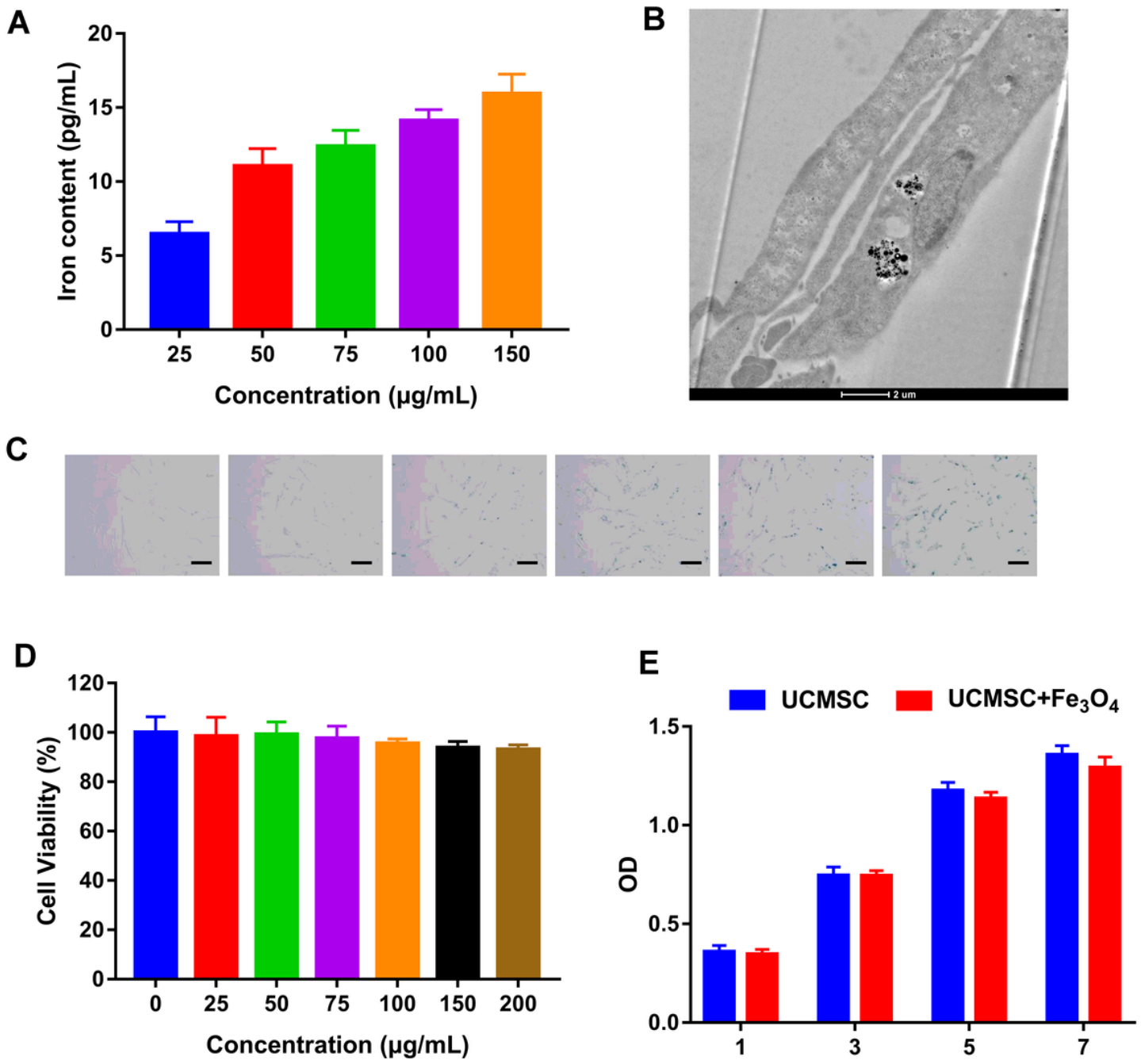

Figure 2

Viability and proliferation of UCMSCs labeled wtih Fe3O4@PDA NPs and internalization of Fe3O4@PDA NPs. (A) The iron concentration in UCMSCs was measured by ICP-OESA. (B) TEM image of nanoparticles (50μg/mL) in UCMSCs. The red arrow indicated that the nanoparticles phagocytosed by UCMSCs were located in the cytoplasm. (C) UCMSCs were labeled with different concentrations of Fe3O4@PDA NPs (25, 50, 75, 100 and 150μg/mL) for 24h, then UCMSCs stained with a Prussian blue iron stain kit. The scale bar is 100μm. (D) UCMSC viability was detected by CCK-8 assay after treated with different concentration of Fe3O4@PDA NPs s, data were normalized to control group. All bars represent mean ± SD. (E) Proliferation of the UCMSCs labeled with the Fe3O4@PDA NPs (50 μg/mL) for 1, 3, 5, and 7 days.

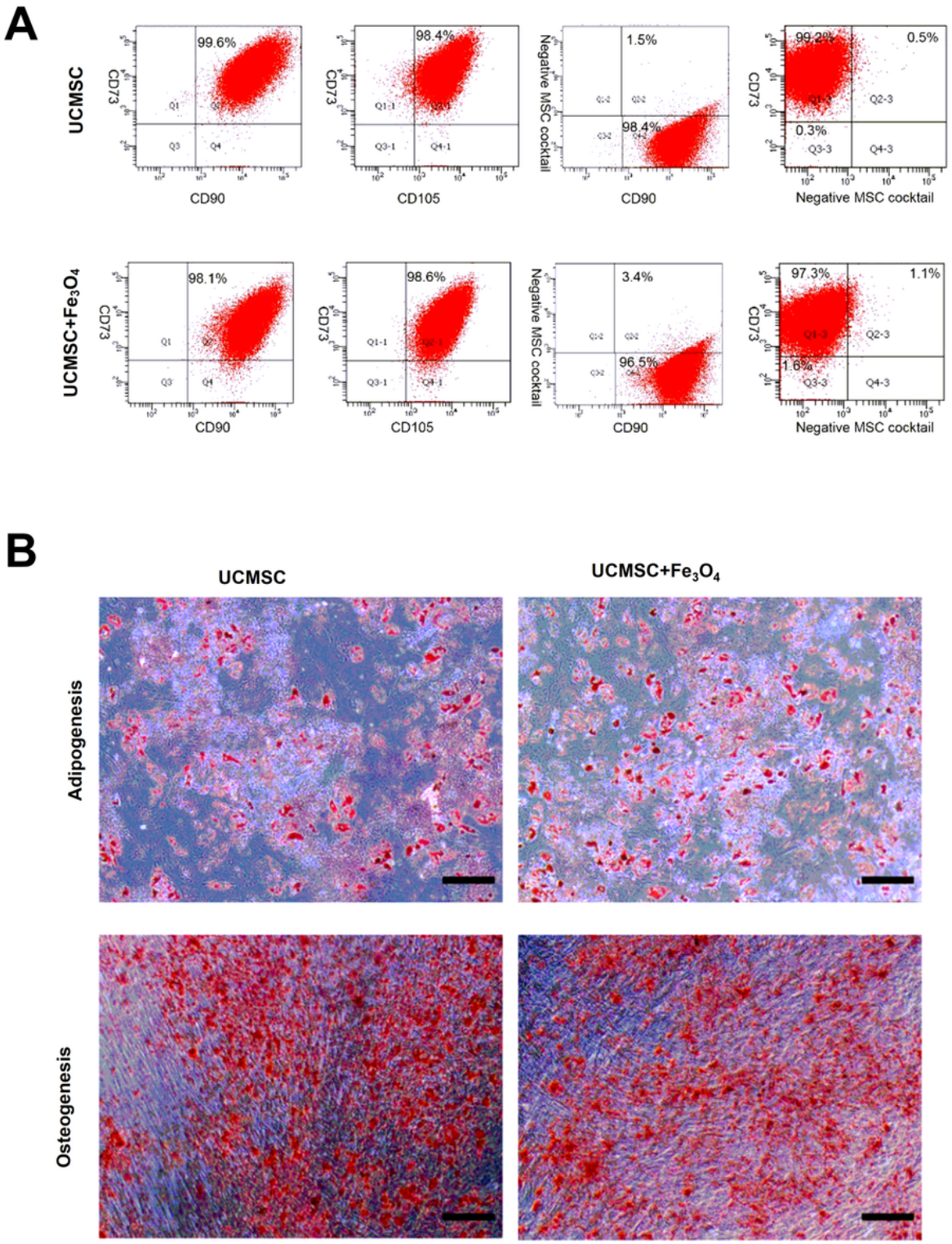

Figure 3

Impact of Fe3O4@PDA NPs on UCMSC functionality. (A) Flow cytometry analysis of UCMSC labeled with Fe3O4@PDA NPs showed that they were positive for CD73, CD90 and CD105 and negative for CD19, CD34, CD11b and CD45, HLA-DR. Negative MSC cocktail contained CD19, CD34, CD11b, CD45 and HLA-DR. (B) Differentiation of UCMSC labeled with Fe3O4@PDA NPs in differentiation media. UCMSC labeled

with Fe3O4@PDA NPs showed adipogenic and osteogenic differentiation potential alike UCMSC. Scale bar = 50 μm.

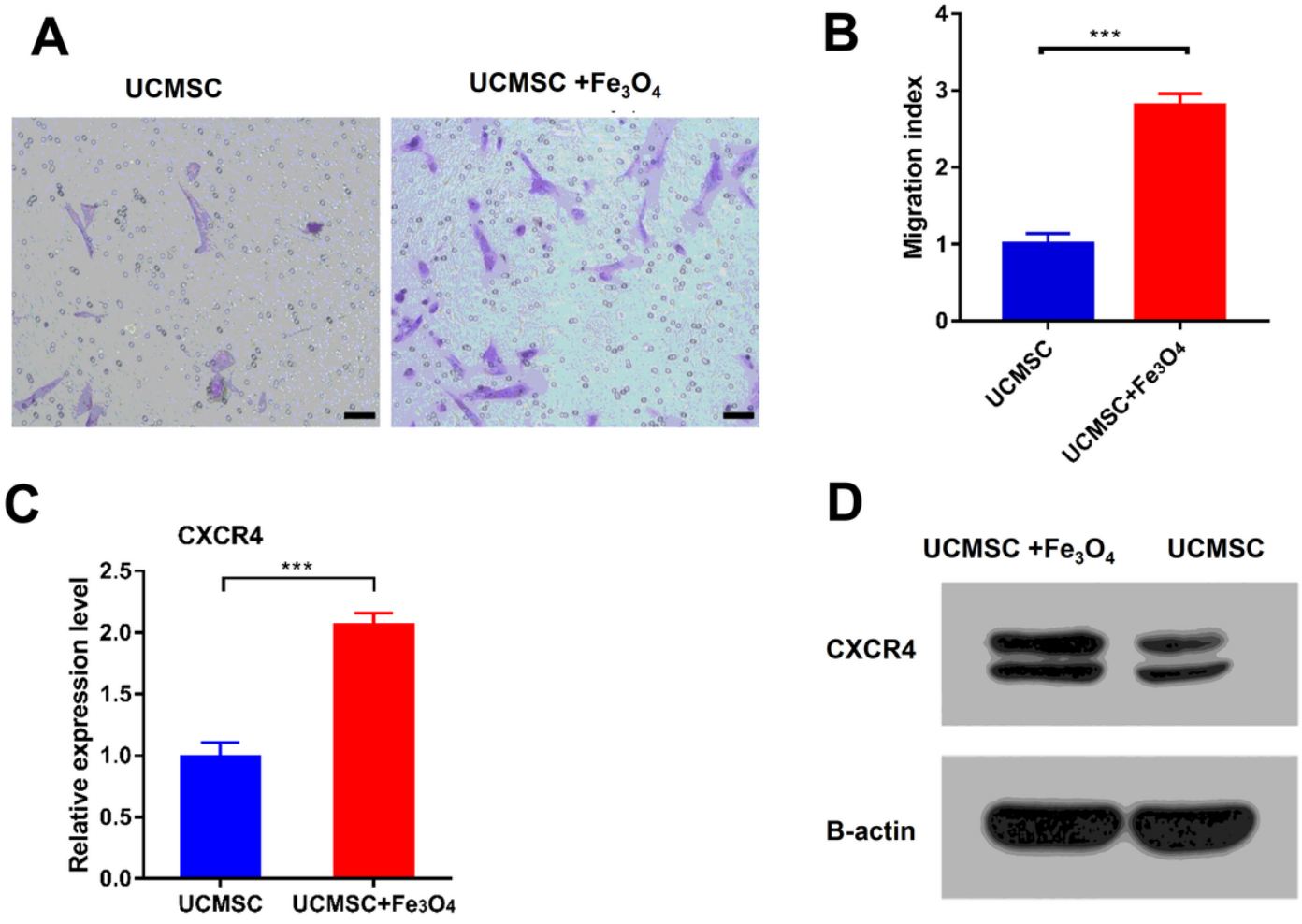

Figure 4

The effect of nanoparticles on the migration of UCMSCs. (A) Transwell experiments evaluated the migratory ability of UCMSC labeled with Fe3O4@PDA NPs and UCMSC. (B) Quantitative analysis of the ratio of the migrated cells in the labeled and unlabeled groups. (C) qRT-PCR analysis of CXCR4mRNA expression in the labeled and unlabeled groups. (D) Western blot analysis of CXCR4 protein expression in the labeled and unlabeled groups. ***P < 0.001. Scale bar =100 μm.

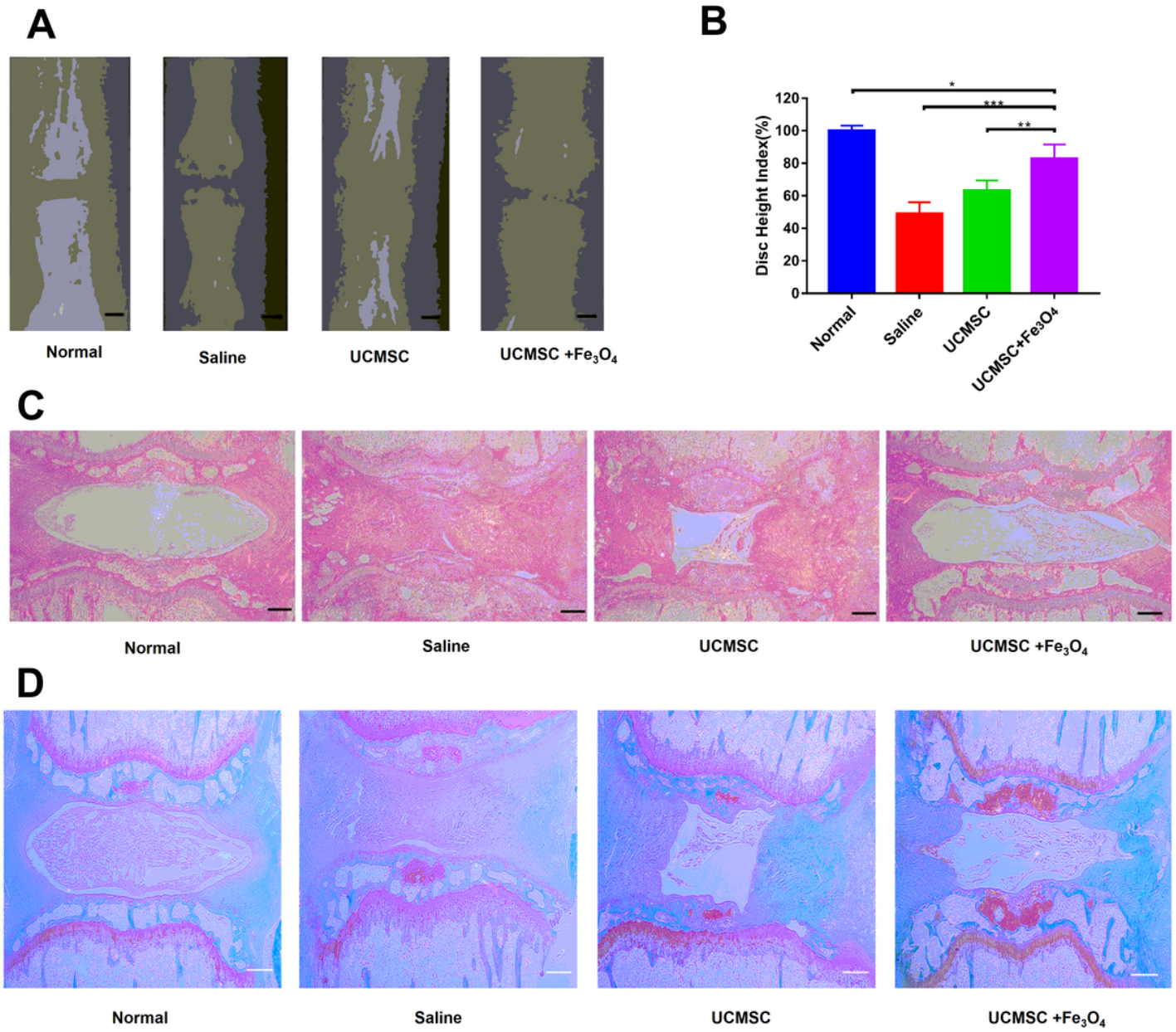

Figure 5

In vivo radiographic changes and histological evaluation of the effect of UCMSC labeled with Fe3O4@PDA NPs on the repair of intervertebral disc. (A) Representative rat tail X-ray image in each group, Scale bar=2mm. (B) Disk height index (DHI) of the disk from different groups at 2 weeks after surgery. n =3. (C) H&E staining was shown in a representative longitudinal section of the intervertebral disc and adjacent vertebrae. Scale bar= 500μm. (D) Safranin-O/fast green staining of intervertebral discs isolated from different groups. Scale bar= 500μm. *P < 0.05, **P < 0.01, ***P < 0.001.

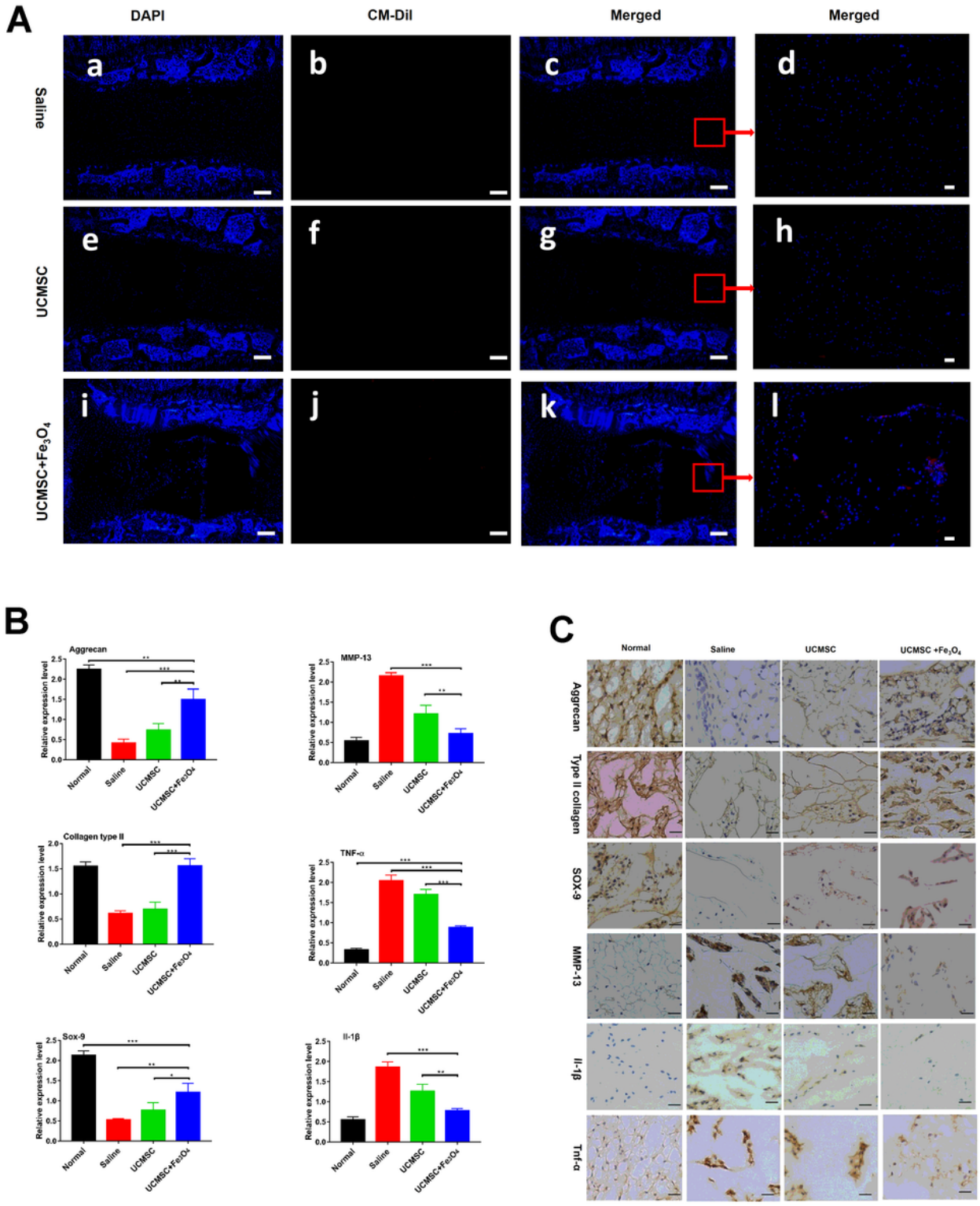

Figure 6

UCMSC migration in degenerated IVD and gene expression and immunohistochemical analysis of the effect of UCMSC labeled with Fe3O4@PDA NPs on the repair of intervertebral disc.
(A)Immunofluorescence showed the survival and migration of UCMSCs 2 weeks after cell transplantation. (a–d) showed the saline group. (e–h) showed UCMSCs group. (i–l) showed the Fe3O4@PDA NP labeled UCMSC group. (a-c), (e-g), (i-k) scale bar = 200 nm. (d,h,i) scale bar = 100 nm. (B)

Real-time quantitative polymerase chain reaction gene expression analysis of aggrecan, type II collagen, Sox-9, Mmp-13, Tnf-α and Il-1β in control, saline, UCMSC and Fe3O4@PDA NPs labeled UCMSC group at 2 weeks postinjection. Data is expressed as the relative fold-change to the control and normalized to GAPDH. (C) Typical immunohistochemical images of the major IVD matrix proteins at 2 weeks postinjection. IVD sections were labeled with aggrecan, type II collagen, Sox-9, Mmp-13, Tnf-α and Il-1β antibodies. Scale bar = 25 μm. *P < 0.05, **P < 0.01, ***P < 0.001.

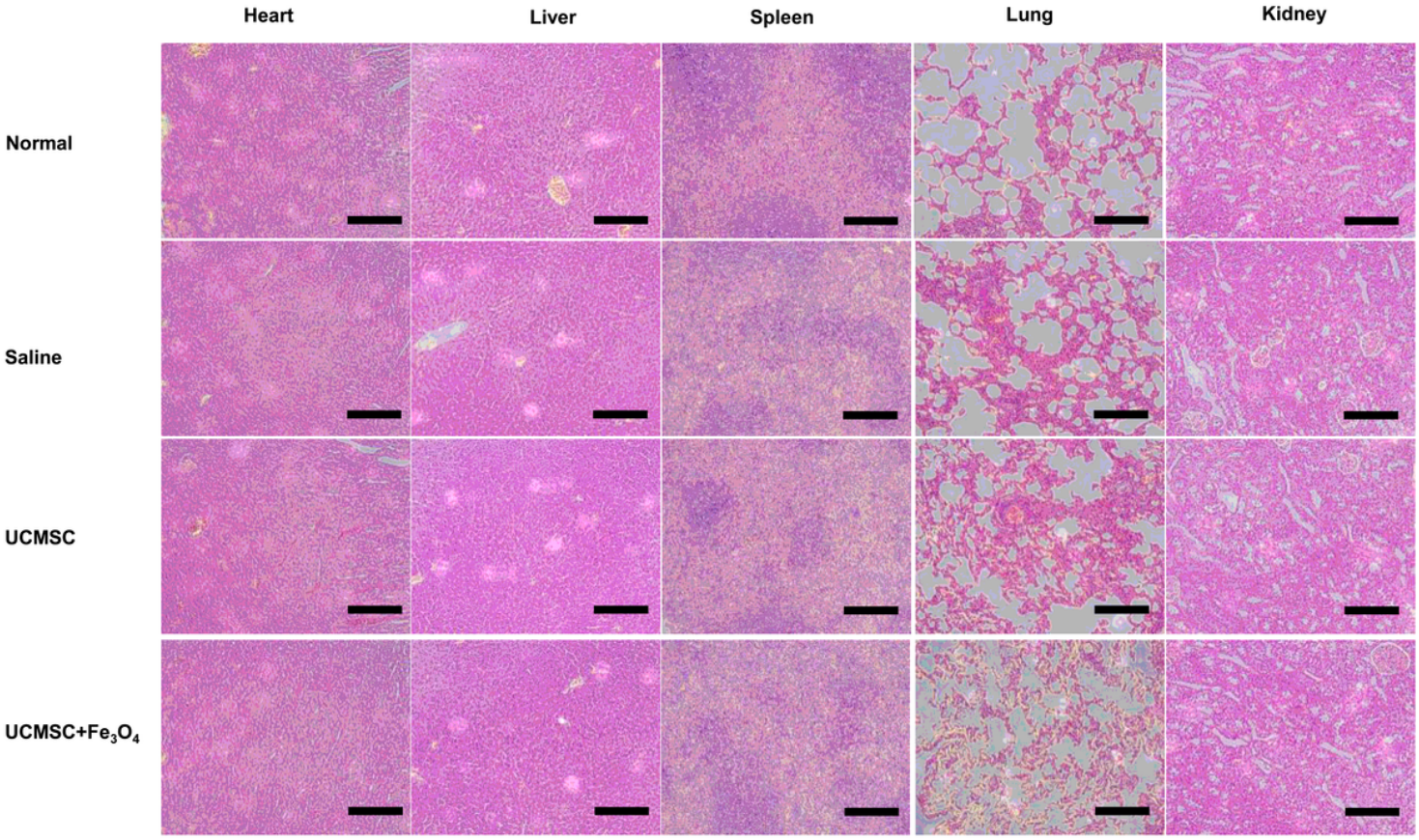

Figure 7

H&E staining analysis of the major organs of mice from the different groups after 2 weeks of treatment, Scale bar = 100 μm.

Supplementary Files

This is a list of supplementary files associated with this preprint. Click to download.

- OnlineGraphicalAbstract.png